Novel Techniques for Investigating the High Temperature Degradation of Protective Coatings on Nickel Base Superalloys

A.A.Alibhai, D.P Garriga-Majo, B.A Shollock, D.S. McPhail

Department of Materials, Imperial College of Science, Technology and Medicine,
Prince Consort Road, London, SW7 2BP

Abstract

In order to facilitate improved fuel efficiency and power to weight performance in gas turbines, components are subjected to increasing operating temperatures. The demanding operating conditions have lead to the development of coating systems, which protect the gas turbine components from environmentally induced attack. The effectiveness of the coating relies on the mechanism by which a healing oxide scale is formed and replaced during thermal cycling. Therefore, in order to optimise coating performance, it is vital to develop a clear understanding of the oxidation mechanisms involved during scale formation. [1]

Novel approaches involving $^{18}O_2$ isotopic tracer experiments, secondary ion mass spectrometry (SIMS) and focused ion beam (FIB) in-situ milling, have been employed to investigate the high temperature oxidation mechanisms of various commercial protective coatings on industrial gas turbines and other nickel base superalloy systems. These techniques lend themselves well to the study of high temperature degradation, as they are able to provide essential information on the diffusion pathways of oxygen anions and metal cations during oxide formation [2-3].

In the first part of this study, the use of a two-stage tracer oxidation technique and Secondary Ion Mass Spectrometry have been employed to investigate the oxygen diffusion mechanisms occurring during scale formation on uncoated superalloys CMSX4 and CM186LC at temperatures between 826°C to 1100°C.

The cation depth profiles obtained give information regarding the chemical nature of the oxides formed and these results provide a baseline against which the oxidation performance of coatings may be assessed.

In the second part of this study, oxides formed on a platinum aluminide coating MDC150L which had been oxidised at 870°C, have been analysed by micromaching cross sections of the oxide layer using a Ga^+ focused ion beam (FIB-FEI Europe) instrument. These cross sections were analysed on the FIB, using secondary ion and electron imaging, and oxygen mapping.

Results from this study have provided essential information regarding the microstructural evolution of the oxide layer during high temperature exposure, revealing the oxide thickness and isotopic oxygen distribution. For uncoated superalloy CM186LC, outward cation diffusion was observed for all temperatures between 820°C and 1100°C. In the case of superalloy CMSX4, outward cation diffusion occurred at temperatures up to 996°C. Above 996°C a change in mechanism was observed and combination of outward cation and inward oxygen diffusion occurs. For the coating system MDC150L, outward cation diffusion is observed at 870°C, for extended oxidation periods up to 82 hours, and the coating formed an effective alumina scale.

These encouraging results obtained have highlighted the usefulness of the focused ion beam technique and secondary ion mass spectroscopy in elucidating the high temperature degradation of protective coatings and nickel base superalloys.

Introduction

Thermal barrier coating (TBC) systems are typically applied to hot section components of gas turbine engines in order to reduce part temperatures and improve component durability. TBC systems involve a ceramic top coat, which is most commonly yttria–stabilised zirconia (YSZ) due to its poor thermal conductivity and good coefficient of thermal expansion. An underlying metallic bond coat is applied between the superalloy substrate and the ceramic top coat. This bond coat must be resistant to high temperature oxidation as the ceramic top coat does not act as a barrier to oxygen and hence does not protect the substrate alloy. The metallic bond coat is designed to form a protective and adherent α-Al_2O_3 scale. Spallation of this thermally grown alumina scale leads to the loss of the ceramic top coat and ultimately failure of the TBC system. Various studies [4–6] have shown that the oxidation mechanism of the metallic bond coat is a key aspect in determining the useful lifetime of TBC systems.

The use of isotopic tracer experiments and conventional Secondary Ion Mass Spectrometry (SIMS) has extensively been reported for the study of high temperature oxidation [7], especially for alumina forming systems [2,8-12]. These studies, combined with results obtained from other techniques such as X-Ray diffraction, Rutherford Backscattering Spectrometry and Transmission Electron Microscopy [13-14], have emphasised the possible complexity of the oxide scale growth mechanism, which may involve oxygen and/or cationic diffusion through different pathways and also phase transformations within the oxide scale.

Focused Ion Beam (FIB) technology has recently been applied to the investigation of the high temperature degradation of industrial turbine blades [15] and coatings [16]. FIB technology is routinely used within the semiconductor industry and has only recently been used in other application areas such as specimen preparation for biological electron microscopy [17], multilayer optical oxide/nitride films, hard carbide coating on tool steels [18], and Al-Li-Cu quasicrystal investigations [19]. A major advantage of the application of the FIB system to the study of high temperature oxidation is its capability to perform *in situ* micro-machining (ion milling) of the specimen and to prepare cleaned surfaces for high resolution SIMS analysis and imaging.

The recent developments in high Z-resolution microscopes such as the Atomic Force Microscope and Interferometric Optical Microscopes have made it possible to obtain valuable information regarding the oxide surface properties as well depth calibration of the SIMS craters.

In this paper, novel approaches towards investigating the high temperature oxidation of uncoated superalloys and coating systems are introduced. Investigation of uncoated substrate alloys is useful as it provides information regarding the durability of the bare superalloy in the event of coating failure. It also provides a foundation on which the oxidation performance of coatings may be assessed. In this study, the high temperature isothermal oxidation of uncoated single crystal CMSX4 (Cannon Muskegon) and directionally solidified alloy CM186LC (Cannon Muskegon) were investigated using the two-stage isotopic tracer technique and SIMS analysis. Oxide scales formed on a platinum modified aluminide coating MDC150L (Howmet-Thermatech) were analysed using a focused ion beam system (FIB200) and micromaching cross-sections of the oxide. Analysis of the oxide layer was performed using secondary electron and secondary ion imaging, oxygen mapping and depth profiling.

Experimental Procedure

Materials

Uncoated superalloys CMSX4 and CM186LC were studied at oxidation temperatures between 826°C and 1100°C for a total of 22 hours. These alloys have virtually the same chemical composition, with small differences in elements added to aid the directionally solidified process. Table 1 gives the chemical composition of these superalloys.

A platinum modified aluminide coating MDC150L applied to the directionally solidified alloy CM186LC using a low aluminium activity- chemical vapour deposition process [20] was also investigated for various oxidation periods at 870°C. This coating has a single phase (Ni,Al)Pt additive layer. Beneath this is a well developed diffusion zone, which is almost one third of the total coating thickness, and is characteristic of an outward grown coating. Typically, the total coating thickness (post heat treatment) is 77.5µm and the coating composition is 19.5wt.%Al and 19.0wt.%Pt.

Specimen preparation

In the case of the uncoated superalloys samples were cut with specimen orientation normal to the <100> plane. For alloy CM186LC, specimen orientation was determined via X-Ray Diffraction texture analysis using the Phillips X'Pert Materials Research Diffractometer (MRD). In the case of the single crystal alloy CMSX4, back reflection Laue was performed using a 30kV voltage and a 30mm film to specimen distance. Samples were then sliced normal to the <100> plane using the Accutom 5 cutting machine (Struers). Samples were then polished to 1 µm and cleaned ultrasonically in acetone for 20 minutes.

The MDC150L/CM186LC system was received as a fatigue test specimen, which had previously been oxidised for 20 hours in air at 870°C. Small samples were cut for analysis as described above.

Oxidation Study

A two-stage oxidation treatment was performed on all the samples. In this tracer oxidation technique, the sample was first oxidised in one isotope of oxygen with an $^{18}O_2$ partial pressure of g_1, for a period of time t_1, thus forming the first oxide layer. The sample was then oxidised in the tracer isotope with an $^{18}O_2$ partial pressure of g_2 for a period of time t_2, thus forming the new oxide. Uncoated samples CMSX4 and CM186LC were first oxidised for 18 hours in $^{18}O_2$ (enriched to 50%, g_1=0.5), followed by 4 hours in unlabelled $^{16}O_2$ (g_2=0.002), at temperatures between 826°C and 1100°C. The coated samples MDC150L on alloy CM186LC were first oxidised in air (g_1=0.002) for 20 hours at 870°C (as received condition). The samples were then further oxidised in $^{18}O_2$ (enriched to 87%, g_2=0.87) for 4 hours and 62 hours at the same temperature. All oxidations took place at 200 millibar pressure and the sample tube was briefly evacuated between anneals. Table 2 summarises the oxidation treatments and the SIMS and FIB experiments performed on the uncoated superalloys CMSX4 and CM186LC and the coating MDC150L.

ALLOY	COMPOSITIONAL DATA (wt %)												
	Ni	Hf	C	Cr	Co	Mo	W	Re	Ta	Al	Ti	B	Zr
CM186LC	bal	1.4	0.07	6.0	9.0	0.5	8.4	3.0	3.4	5.7	0.7	0.015	0.015
CMSX4	bal	0.1	0.1	6.5	9.0	0.6	6.0	3.0	6.5	5.6	1.0	-	-

Table 1: Compositional Data (wt%) for alloys CMSX4 and CM186LC, which were investigated in the two-stage isotopic oxidation study.

Secondary Ion Mass Spectroscopy

SIMS depth profiling is an extremely useful technique for analysing the tracer oxygen diffusion mechanisms in metal systems, as it is able to distinguish all the isotopes in the periodic table. Although this is a destructive surface analysis technique, it combines very high depth resolution with exceptional detection limits (typically parts per million). This technique involves a mono-energetic focused beam of primary ions (typically 0.25keV to 15keV), bombarding the surface of a solid sample in a vacuum. The momentum transfer between the incoming ions and the constituent atoms leads to the emittance of secondary species from the surface of the material. This process is known as sputtering. The sputtered species may be neutral or charged particles. The charged particles are detected and analysed using conventional mass spectrometry analysis. As the ion beam continually rasters across the surface of the sample, it sputters material from the surface thus forming a square crater.

In this study SIMS depth profiling measurements were conducted on the oxidised superalloy samples using the ATOMIKA 6500 Ion Microprobe. A Xenon (Xe^+) primary ion beam was used to raster the surface of the sample at near normal incidence, with a primary beam energy of either 8keV or 15keV. Negative secondary ions of $^{16}O^-$ and $^{18}O^-$ were monitored as a function of time for all samples. During analysis of the uncoated samples, metal ions such as $^{27}Al^-$, $^{59}Co^-$, $^{58}Ni^-$ and $^{52}Cr^-$ were also monitored. Scan widths of between 250µm and 300µm were employed and secondary ions were gated to 25% of the total raster area in order to avoid any crater wall effects.

The Focussed Ion Beam System

The focussed ion beam system (FIB200-FEI UK Ltd.) works in essentially the same manner as conventional SIMS, but in this case the FIB200 employs a gallium Ga^+ liquid metal ion source, which operates at 30keV. The size of the beam can be pre-programmed depending on the beam current used and typically a beam diameter of just a few nanometers can be achieved using a current of approximately 1 picoampere. Typically, high currents (few nA) are used to mill different shapes of crater and smaller currents (few pA) permit high resolution SIMS analysis. In order to prevent surface charging a thin layer of platinum (typically 1µm) may be deposited in-situ.

The FIB200 system is equipped with different detectors:
- a secondary electron detector.
- a channeltron (CDEM) used to detect secondary ions and high energy electrons for imaging.
- a quadrupole mass spectrometer for SIMS analysis (mass spectrum, depth profiling, elemental mapping).

The Ga+ primary beam generates a low secondary ion signal compared to conventional ion sources such as O_2^+ and Xe^+, but it offers a very high spatial ability. The different motions of the stage X, Y, Z, rotation and tilt can be followed using an optical camera.

In this study oxides formed on the coated sample MDC150L were analysed by ion milling cross sections of the oxide and performing secondary electron imaging and isotopic oxygen mapping. The oxide surface was coated with platinum in order to avoid any surface charging. Depth profiling using the FIB200 was also performed on all the oxides grown on the coated sample.

Depth Calibration

Depth calibration of the profiles was performed using a Z-high resolution microscope (Zygo) and an Atomic Force Microscope (Quesant Resolver), by measuring the total depth of the craters and assuming a constant sputter rate throughout the oxide scale.

Determination of Tracer Enrichment

In order to be able to compensate for any undesirable variations in secondary ion intensities due to surface charging, the isotopic fractions ir_{18} and ir_{16} are plotted as a function of depth. Neglecting any contribution from $^{17}O^-$, which has a natural abundance of 0.037%, the isotopic fractions for oxygen 18 and oxygen 16 are given as: $ir_{18} = \dfrac{^{18}O^-}{^{18}O^- + ^{16}O^-}$ and $ir_{16} = 1 - ir_{18}$ respectively.

These isotopic fractions reflect the actual isotopic concentration variations in the oxide scale. In order to quantify the relative isotope tracer enrichment in the oxide scale, the parameter v was estimated for the oxidation treatments performed and is given by:

$$v = \frac{ir_{18} - g_1}{g_2 - g_1}$$

where g_1 and g_2 are the $^{18}O_2$ partial pressure in the first and second oxidation atmospheres respectively. By plotting the tracer enrichment parameter v as a function of depth, it is possible to distinguish the regions where the new oxide has grown. Regions of pure new oxide growth have a v-value of unity, whereas regions of old oxide growth have values of zero. Regions that contain a mixture of new and old oxide have a v- value between 0 and 1.

Material	Oxidation Treatment					SIMS Machine*	SIMS Depth Conditions
	Temperature (°C/°F)	t_1 (hours)	g_1	t_2 (s)	g_2		
CMSX4	826/1519	18	0.50	4	0.002	Atomika	Xe^+/8keV
CMSX4	906/1663	18	0.50	4	0.002	Atomika	Xe^+/8keV
CMSX4	996/1825	18	0.50	4	0.002	Atomika	Xe^+/8keV
CM186LC	826/1519	18	0.50	4	0.002	Atomika	Xe^+/8keV
CM186LC	906/1663	18	0.50	4	0.002	Atomika	Xe^+/8keV
CM186LC	996/1825	18	0.50	4	0.002	Atomika	Xe^+/8keV
CM186LC	1100/2012	18	0.50	4	0.002	Atomika	Xe^+/8keV [†]
CM186LC+MDC150L	870/1598	20	0.002	-	-	Atomika	Xe^+/15keV
CM186LC+MDC150L	870/1598	20	0.002	4	0.87±0.02	Atomika	Xe^+/15keV[†]
CM186LC+MDC150L	870/1598	20	0.002	62	0.87±0.02	FIB200	Ga^+/30keV
CM186LC+MDC150L	870/1598	20	0.002	62	0.87±0.02	FIB200	Ga^+/30keV

Table 2: Summary of oxidation treatments and SIMS/FIB analyses performed on alloys CMSX4, CM186LC, CM186LC and coating system MDC150L. An electron [...] used to ensure charge compensation on these samples. *Atomika refers to the Atomika 6500 Ion Microprobe and FIB200 refers to the Focused Ion Beam [...]

678

Depending on the oxidation temperature and the superalloy substrate, the diffusion of the tracer and the further growth of the oxide may take place at one of these three locations:

1. At the gas/oxide interface with a new oxide growth of thickness d_g.
2. Within the oxide formed during the first thermal treatment, the thickness of this new oxide layer is called d_o.
3. At the oxide/metal interface with a new growth of thickness d_m.

The total oxide thickness is typically determined by the depth over which the sum of the two negative oxygen secondary ion intensities falls to half its maximum value and is denoted as $d_{0.5}$. An example of this is given in figure 1 for alloy CMSX4 oxidised at 996°C and values of $d_{0.5}$ are given in table 3.

The cation diffusion mechanisms are presented as normalised secondary ion intensities. These are determined by dividing the negative metal secondary ion count rate at profiling time t over the maximum negative secondary ion count rate for that metal species. This method allows the relative variation of each metal species in the oxide to be displayed. Examples of cation depth profiles for CM186LC and CMSX4 oxidised at 996°C for total oxidation periods up to 22 hours are given in figures 2 and 4.

Results

Uncoated Superalloys

Values for the total oxide thickness $d_{0.5}$ and regions of new and partially new tracer oxide thickness at the gas/oxide interface (d_g), metal/oxide interface (d_m) and within the existing oxide (d_o) are given in Table 3, as well as the predominant oxidation mechanisms that occur in superalloys CMSX4 and CM186LC which have been oxidised for 18 hours in $^{18}O_2$, followed by 4 hours in $^{16}O_2$. The average oxide growth rate for these superalloys for each temperature has been determined by dividing the total oxide thickness $d_{0.5}$, by the total oxidation time, which is 1320 minutes (22 hours) in all cases. The oxygen depth profile for alloy CMSX4 oxidised at 996°C, for 18 hours in $^{18}O_2$, followed by 4 hours in $^{16}O_2$ is shown in figure 1.

The depth over which the sum of the oxygen 18 and oxygen 16 ions falls to half its maximum value, is one possible method of determining the total oxide scale.
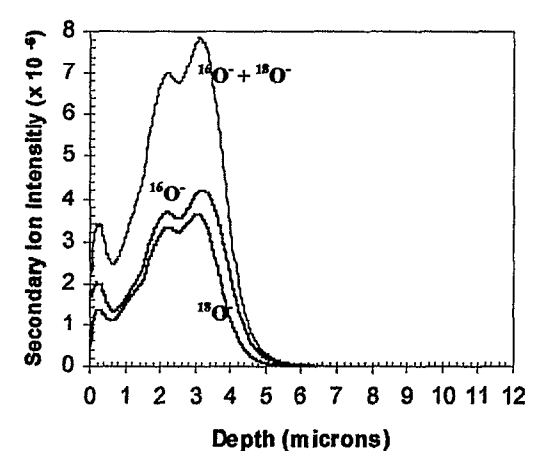

Figure 1: Oxygen depth profile for sample CMSX4 oxidised at 996°C. The total oxide thickness $d_{0.5}$ occurs at 4.2μm, which is the depth at which the sum of the $^{18}O^-$ and $^{16}O^-$ falls to half its maximum

Alloy	Oxidation Temperature (°C)	Total Oxide Thickness $d_{0.5}$ (μm)	Average Growth Rate (nm/min)	New Oxide Growth			Oxidation Mechanism
				d_g (μm)	d_o (μm)	d_m (μm)	
CMSX4	826	1.2	0.91	0.1	-	-	
CMSX4	906	3.2	2.42	0.15	1.0	-	Outward Cation Diffusion
CMSX4[†]	996	4.2	3.71	0.5	-	1.0	Combination of Outward Cation and Inward Oxygen Diffusion
CM186LC	826	1.4	1.06	0.2	-	-	
CM186LC	906	5.5	4.17	1.2	-	-	Outward Cation Diffusion
CM186LC[‡]	996	7.0	5.30	1.6	-	-	
CM186LC	1100	12.0	9.0	4.8	-	-	

Table 3: Summary of results for CMSX4 and CM186LC showing where the tracer oxide has formed and predominant oxidation mechanism. [†] Cation depth profiles and tracer enrichment profiles for CM186LC for these conditions are shown in figures 2 and 3 respectively. [‡] Cation depth profiles and tracer enrichment profiles for CMSX4 for these conditions are shown in figures 4 and 5 respectively.
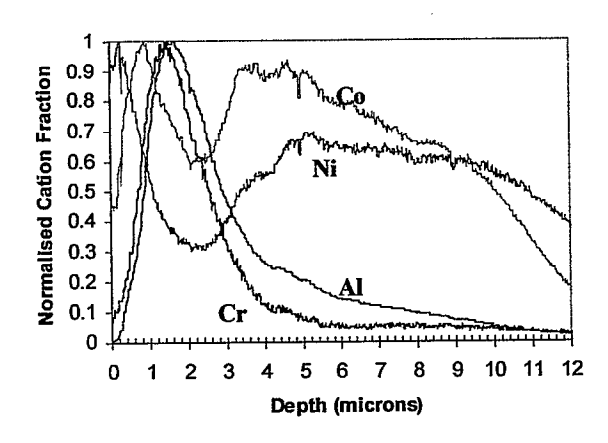
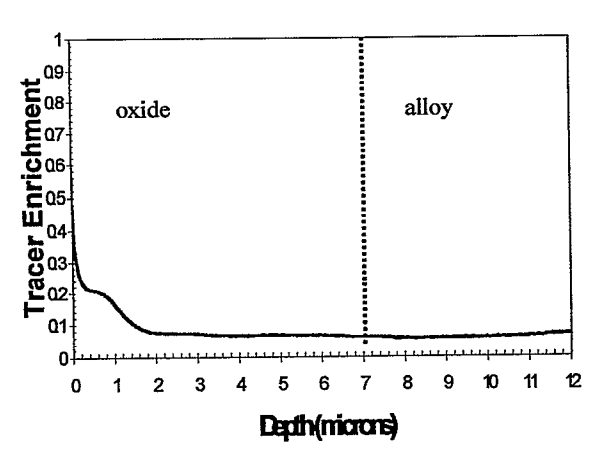Figure 2: Normalised cation depth profile for CM186LC oxidised at 996°C for 18 hours in $^{18}O_2$ and 4 hours in $^{16}O_2$.
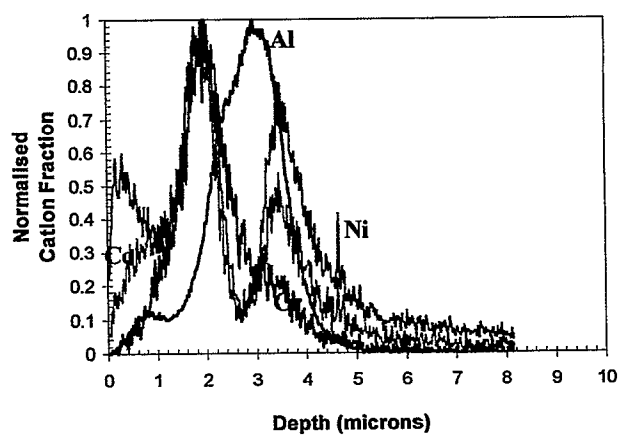

Figure 4: Normalised cation depth profile for CMSX4 oxidised at 996°C 18 hours in $^{18}O_2$ and 4 hours in $^{16}O_2$.

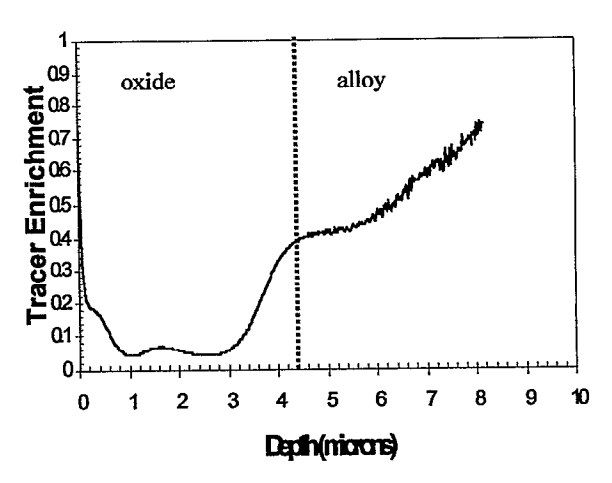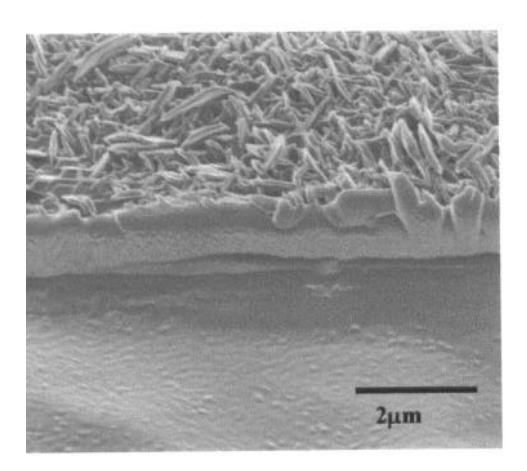Figure 3: Tracer enrichment profile for CM186LC oxidised at 996°C as for figure 2.

Figure 5: Tracer enrichment profile for CMSX4 oxidised at 996°C as for figure 4.

Coating MDC150L

Total oxide thickness $d_{0.5}$, average oxide growth rate and the predominant oxidation mechanism that occurs for the coating system MDC150L at 870°C for oxidation in air for 20 hours and various periods up to 62 hours in $^{18}O_2$ are given in Table 4.

Oxidation Time (hours)	Total Oxide thickness (μm)	Average Growth Rate (nm/min)	Predominant Oxidation Mechanism
20 hours air	0.5	0.41	Outward Cation Diffusion
20 hours air + 4 hours $^{18}O_2$	0.55	0.39	Outward Cation Diffusion
20 hours air + 4 hours $^{18}O_2$	0.95	0.19	Outward Cation Diffusion

Table 4: Summary of results obtained for coating MDC150L oxidised at 870°C.

Imaging results from the focused ion beam study for the coating MDC150L which had been oxidised in air for 20 hours and then 62 hours in $^{18}O_2$ at 870°C are given in figures 6 and 8 to 11. The oxide morphology is shown in figure 6, which is a secondary electron image of the crater wall formed after depth profiling. Figure 7 is a schematic diagram showing the direction the gallium beam during in-situ ion milling and imaging which was used to obtain figures 8 to 11. Figure 8 is a secondary ion image of the surface of the oxide formed on the coating, and the position of the wedge crater, which was formed using the Ga^+ beam. The oxide surface above the crater was coated with platinum in order to avoid any surface charging effects. This also helps to clearly define the top of the oxide surface. Figure 9 is a secondary electron image and is an enlargement of the grain boundary area shown figure 8. Figures 10 and 11 are $^{16}O^-$ and $^{18}O^-$ maps respectively and correspond to the same region shown in figure 9.

Figure 6: Secondary electron image of the crater wall formed after depth profiling revealing a θ-Al$_2$O$_3$ whisker morphology on the oxide surface.

Figure 7: Schematic diagram showing the direction of the Ga$^+$ ion beam during in-situ ion milling and imaging.
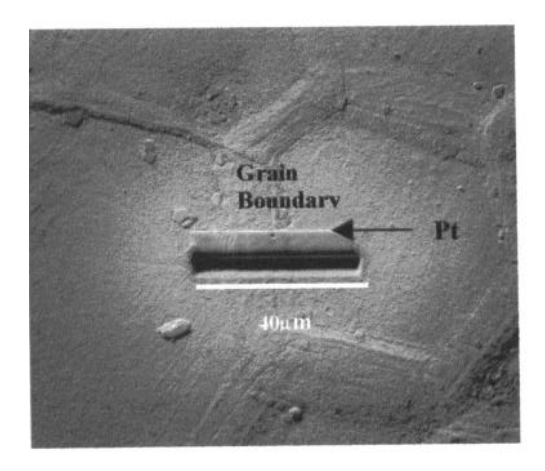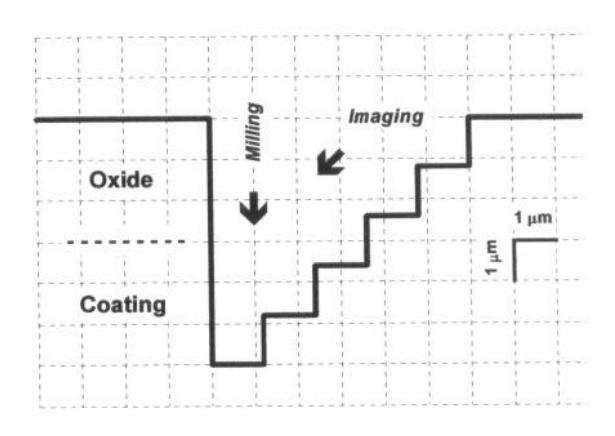

Figure 8: Secondary ion image of the ion-milled crater made on the oxide formed on coating MDC150L oxidised at 870°C for 20 hours in air plus 62 hours in ^{18}O$_2$. Platinum was deposited above the crater in order to avoid any surface charging effects. The hexagonal grain structure of the coating can also be seen.

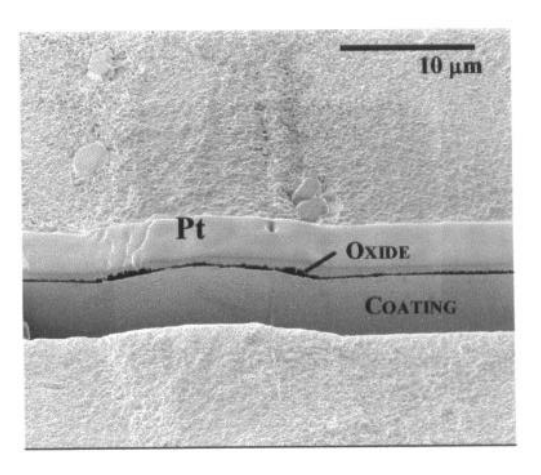Figure 9: A general view of the milled cross-section. (Secondary electron image, tilt 45°).

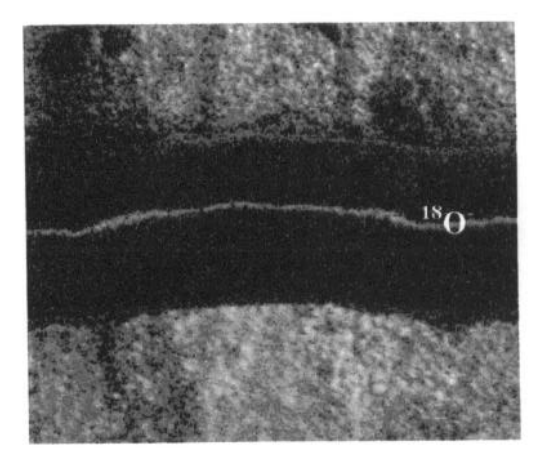Figure 10: ^{16}O$^-$ elemental map over the grain boundary region shown in figure 6.

Figure 11: ^{18}O$^-$ elemental map over the same region as shown in figure 8.

Discussion

Uncoated Superalloys

With respect to the tracer oxidation study made on the uncoated superalloys CMSX4 and CM186LC (given in figure 2 and 3), a number of key observations can be made. Results for alloys CM186LC show that outward cation diffusion is the predominant oxidation mechanism for all temperatures between 826°C and 1100°C. This is shown in the example given in figure 3. The tracer enrichment parameter v is high at the gas-oxide interface indicating possible surface exchange and new oxide growth. Also, with the exception of the oxide formed at 826°C, the total oxide thicknesses are significantly greater for the directional solidified alloy CM186LC compared to those grown on the single crystal alloy CMSX4. Samples for both these superalloys have been cut normal to the <100> orientation and hence this result may be attributed to fast oxygen diffusion down grain boundaries in the directional solidified alloy CM186LC. Such a result is comparable to hot oxidation tests performed by others [22-23] on these alloys.

With respect to the total oxide thickness values $d_{0.5}$ given in tables 3 and 4, it is important to note that this value often gives an underestimate of the true oxide thickness as can be seen for alloy CM186LC, which has been oxidised at 996°C. The $d_{0.5}$ value for this sample is found to be 7.0μm, although the cation diffusion profile at this point is still in the nickel and cobalt plateau. An alternative method for determining the total oxide thickness would be to evaluate the regions of new and old oxide growth at the gas-oxide, old oxide, and oxide-metal interface from the tracer enrichment profile. However, as it is not always possible to determine the oxide growth at the oxide-metal interface (as shown in figure 3), this method is limited. Hence, the total oxide thickness $d_{0.5}$ found from the sum of the oxygen profiles remains an adequate method for determining the total oxide thickness.

The cation diffusion profiles for this alloy also provide interesting information with regard to the nature of the oxides that form. Figure 2 is an example of a normalised cation diffusion profile obtained for this alloy at 996°C. This shows that the oxide at the gas-oxide interface is nickel rich and most likely to be NiO. A middle oxide layer is cobalt rich and the rest of the oxide near the oxide-alloy interface is rich in aluminium and chromium. The nickel plateau observed at depths greater than 5μm indicates a third extended oxide region, which is also rich in cobalt. Although the SIMS technique does not provide quantitative information on the oxide composition, such cation diffusion depth profiles are very useful as they provide information regarding the nature of the oxide formed.

The results obtained for CMSX4 show that a change in oxidation mechanism is observed at 996°C. At lower temperatures, this alloy displays outward cation diffusion. However, at 996°C the mechanism is altered and a combination of inward oxygen and outward cation diffusion through the first oxide layer is observed. Figure 5 shows the tracer enrichment profile for this alloy, which has been oxidised at 996°C. This shows an area of high tracer enrichment at the gas–oxide interface and represents a new growth in this region. It is also interesting to note that in figures 3 and 5 the tracer enrichment does not fall to zero, which may simply represent background enrichment. However, it is plausible that this may correspond to the tracer having exchanged into the previous oxide grains or formed a new phase within the previous oxides grain boundaries. Such behaviour is as predicted by others [21], who have performed such two stage isotopic tracer experiments on alumina forming alloys. The tracer enrichment value then increases to a plateau with a v -value of 0.42, which indicates a region of new oxide growth within the existing oxide. At the oxide-metal interface the tracer enrichment value begins to rise as $^{16}O_2$ gas has been used as the tracer gas. The noise in the rising tail of the profile is characteristic of profiling into the substrate alloy.

The normalised cation depth profile in figure 4 for alloy CMSX4, which has been oxidised at 996°C shows that the region closest to the gas oxide surface is nickel rich, indicating nickel cation diffusion through the oxide to this interface. The central oxide is a mixture of nickel, cobalt and chromium oxide, beneath which a large region of an aluminium rich oxide exists. All the normalised cation fractions tail off towards zero and indicate profiling into the substrate. This is due to the fact that during the SIMS depth profiling, ionisation of the negative cation species takes place more readily in the oxide compared to the superalloy substrate and so low secondary ion counts are obtained in the substrate.

A key observation to be made from these results is that for both superalloys investigated in this study, neither alloy formed a protective alumina or chromia scale and therefore they are likely to degrade rapidly without a protective coating.

Coating MDC150L

Comparison of the oxide scales formed on the coating system MDC150L and uncoated alloy CM186LC reveals that the oxide layer is much reduced for the coating system, even for extended total oxidation periods up to 82 hours. At 870°C, the thickness of the oxide growth on the coating was found to be 0.95μm for an oxidation period of 82 hours, whereas at 826°C, the uncoated CM186LC formed an oxide of thickness 1.2μm for an oxidation period of 22 hours. This is because the coating system is able to form a protective Al_2O_3 scale, which acts as a barrier against the highly damaging environment. Table 4 shows that the average oxide growth for the alumina scale that forms on the coating drops from 0.50nm/min for a total oxidation period of 20 hours, to 0.19nm/min for a total oxidation period of 82 hours. This drop in oxide growth rate indicates the effectiveness of the alumina scale to as a barrier to further oxidation.

The high resolution imaging and isotopic oxygen mapping performed using the FIB200 provided direct characterisation of the oxidation growth mechanisms that occur at 870°C in 20 hours in air and 62 hours in oxygen 18. Figure 6 is a secondary electron image of the crater wall that has formed after depth profiling. This reveals the whisker like surface morphology which is characteristic of θ-Al_2O_3 and has been observed by others [24]. Figure 8 is a secondary ion image showing the ion milled crater on the oxidised surface and the platinum deposit. The oxygen 16 and oxygen 18 maps are shown in figures 10 and 11
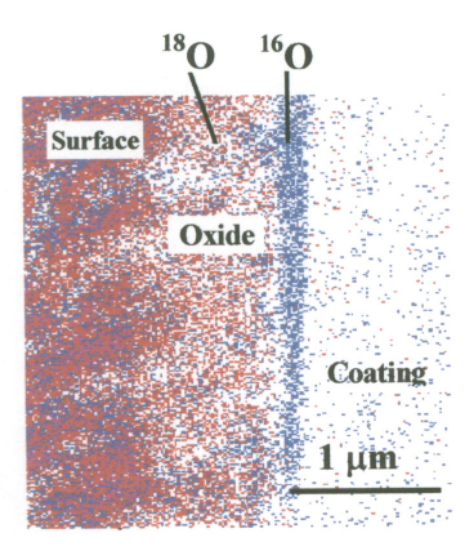
682

Figure 12: MDC150L Isotopic Ratio Map
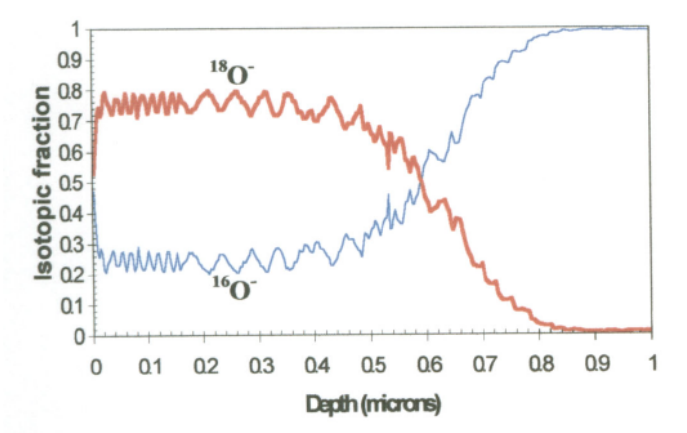Oxidation for: 20 hours in air + 62hours in $^{18}O_2$ at 870°C.

Figure 13: Isotopic Ratio Profile for coating MDC150L obtained via depth profiling for sample oxidised as above. The isotopic fractions are given by: $ir_{18} = \dfrac{^{18}O^-}{^{18}O^- + ^{16}O^-}$ and $ir_{16} = 1 - ir_{18}$.

The isotopic ratio map that is shown in figure 12 above was determined directly from the oxygen 16 and oxygen 18 maps. The FIB oxygen mapping technique provides very localised information regarding the oxidation mechanism of a very specific area of interest and can be used to compare any isotopic oxygen difference in the oxide scale formed at the coating grain and grain boundary. The results obtained from the isotopic ratio maps are in good agreement with the isotopic fraction profile that was obtained by depth profiling, which is shown in figure 13. This shows that for oxidation treatments at 870°C, the oxygen 18 isotopic ratio is high at the gas–oxide interface and hence relates to outward cation diffusion. This is true for all the oxidation treatments irrespective of oxidation time.

Conclusion

These promising results obtained have emphasised the usefulness of Secondary Ion Mass Spectroscopy and the Focused Ion Beam technique in elucidating the high temperature oxidation of nickel base superalloys and protective coatings. Alloy CM186LC displayed outward cation diffusion for all temperatures between 826°C and 1100°C, whereas CMSX4 has shown a change in mechanism. At temperatures between 826°C and 906°C, this alloy displays outward cation diffusion, whereas at 996°C a combination of inward oxygen and outward cation diffusion is observed. Neither alloy formed a protective oxide scale. The coating system MDC150L displayed outward cation diffusion at 870°C for oxidation periods up to 82 hours and formed a effective alumina scale. The tracer enrichment profiles that were obtained for the uncoated superalloys provide useful information regarding the oxidation mechanisms that occur during oxide evolution. Their respective cation depth profiles provide detailed information regarding the compositional nature of the thermally grown scale. The high resolution and in-situ milling capabilities of the FIB system have been particularly useful in characterising the oxide formed on the coated system MDC150L. Oxygen isotopic ratio maps give direct information regarding the diffusion mechanism and are free from errors associated with depth calibration of depth profiles.

This encouraging application of secondary ion mass spectrometry and the focused ion beam technique has clearly established the usefulness of such analyses in determining the high temperature oxidation of superalloy materials and protective coatings.

References

[1]T.N. Rhys-Jones, "Protective Oxide Coatings on Superalloys and Coatings Used in Gas Turbine and Vane Applications." Mat. Sci. & Tech,. 4, (1988), 421-430.

[2]J.Jedlinski, G.Borchardt and S. Mrowec, "Transport Properties of Alumina Scales on the β-NiAl Intermetallic" Solid State Ionics, 50, (1992), 67-74

[3]B.A. Pint, J.R. Martin and L.W Hobbs, "^{18}O SIMS Characterisation of the growth mechanism of doped and undoped $α$-Al_2O_3," Oxidation of Metals, 39, (1993), 167

[4]H.M Tawancy, N. Sridhar and N.M Abbas, "Failure Mechanism of a Thermal Barrier Coating on a Nickel-Base Superalloy" Journal of Mat.Sci, 33, (1998), 681-686.

[5]A.M Freborg et al., "Modelling Oxidation Induced Stresses In Thermal Barrier Coatings" Mat Sci & Engineering A, A245, (1998), 182-190.

[6]B.A. Pint et al., "Substrate and Bond Coat Compositions: Factors Affecting Alumina Scale Adhesion" Mat Sci & Eng A, VolA245, (1998) pp.201-211.

[7]H Caspari,. "Protective coatings extend gas turbine life and efficiency." Reprinted from Power Generation Technology (1995) for Sermatech International Inc.

[8]P Sahoo and G.W Goward.: "On the suitability and application of MCrAlY coatings under various operating conditions". Thermal Spray Industrial Applications – (paper presented at the 8th National Thermal Spray Conference, Houston, Texas, September 11-15, 1995), 539-544.

[9]M.J Graham.: "The study of oxide scales using SIMS", Microscopy of Oxidation. Institute of Materials, No. 500, 10-18.

[10]J Doychak.: "Oxidation behaviour of high-temperature intermetallics.," Intermetallic Compounds, (John Wiley & Sons, 1994), vol. 1, chap. 43.

[11] W.J Quadakkers. et al, "Effect of the θ alumina formation on the growth kinetics of alumina-forming superalloys". Oxidation of Metals. 46, (5/6), (1996), 465-480.

[12] G Borchardt., J Jedlinski. and W Wegener, "Oxygen-18 tracer diffusion as a tool to study high temperature oxidation of metals". (In Proceedings of the 8th. Secondary Ion Mass Spectrometry, Amsterdam, The Netherlands, September 15-20th 1991), 737-740.

[13] J Doychak. and J.L Smialek. "Transient oxidation of single crystal β-NiAl". Metal. Trans. 20A, (1989), 499.

[14] P.T Mosely et al,. "The microstructure of the scale formed during the high temperature oxidation of Fecralloy steel" Corrosion. Science., vol. 24, 1984, p. 547.

[15] D.Garriga-Majo et al., "Novel strategies for evaluating the degradation of protective coatings on superalloys" Journal of Inorganic Materials, 1, (1999), 325-336

[16] A.Alibhai, D.McPhail, B.A Shollock, "Use of isotopic tracers and SIMS analysis for evaluating the high temperature degradation of protective coatings on nickel based superalloys" (In Proceedings of the 12th. Secondary Ion Mass Spectrometry, Brussels 1999).

[17] K Robinson et al. "Applications of focused ion beam milling in biological electron microscopy". Microsc. and Analysis., (1997), 15-16

[18]N. Presser and M.R Hilton, "Applications of focused ion beam machining to the characterisation of carbide, nitride and oxide films," Thin Solid Films, 308, (1997), 369-374

[19]F Wang, P Garoche and L Dumoulin, "Focused ion beam imaging of grains in Al-Li-Cu quasicrystal," Journal. Of Physics-Condensed Matter, 10, (16), (1998), 3479-3488.

[20]B.M. Warnes and D. Punola, "Clean diffusion coatings by chemical vapour deposition," Surface and Coatings Technology, 94-95, (1997), 1-6.

[21]S.N.Basu and J.W. Halloran, "Tracer isotope distribution in growing oxide scales," Oxidation Of Metals, 27, (3/4), (1987), 142-155.

[22]P.S. Burkholder et al., "CM186LC alloy single crystal turbine vanes," (International Gas Turbine and Aeroengine congress and exhibition, Indianapolis, Indiana, 7-10 June 1999).

[23]P.S. Korinko, M.J. Barber and M. Thomas, "Coating Characterisation and Evaluation of Directionally Solidified CM186LC and Single Crystal CMSX4," (ASME Turbo EXPO 1996, NEC, Birmingham, UK).

[24]G.C. Rybicki and J.L Smialek, " Effect of the θ-α-Al_2O_3 transformation on the oxidation behaviour of β-NiAl +Zr," Oxidation Of Metals, 31,(3/4), (1989), 275-304.